

# DHOT-GM: Robust Graph Matching Using A Differentiable Hierarchical Optimal Transport Framework

Haoran Cheng<sup>1</sup> Dixin Luo<sup>1\*</sup> Hongteng Xu<sup>2,3</sup>

<sup>1</sup>School of Computer Science and Technology, Beijing Institute of Technology

<sup>2</sup>Gaoling School of Artificial Intelligence, Renmin University of China

<sup>3</sup>Beijing Key Laboratory of Big Data Management and Analysis Methods

## Abstract

Graph matching is one of the most significant graph analytic tasks in practice, which aims to find the node correspondence across different graphs. Most existing approaches rely on adjacency matrices or node embeddings when matching graphs, whose performances are often sub-optimal because of not fully leveraging the multi-modal information hidden in graphs, such as node attributes, subgraph structures, etc. In this study, we propose a novel and effective graph matching method based on a differentiable hierarchical optimal transport (HOT) framework, called DHOT-GM. Essentially, our method represents each graph as a set of relational matrices corresponding to the information of different modalities. Given two graphs, we enumerate all relational matrix pairs and obtain their matching results, and accordingly, infer the node correspondence by the weighted averaging of the matching results. This method can be implemented as computing the HOT distance between the two graphs — each matching result is an optimal transport plan associated with the Gromov-Wasserstein (GW) distance between two relational matrices, and the weights of all matching results are the elements of an upper-level optimal transport plan defined on the matrix sets. We propose a bi-level optimization algorithm to compute the HOT distance in a differentiable way, making the significance of the relational matrices adjustable. Experiments on various graph matching tasks demonstrate the superiority and robustness of our method compared to state-of-the-art approaches.

## 1 Introduction

As one of the most significant tasks in graph analysis, graph matching aims to find the node correspondence across different graphs. With the correspondence between nodes, the common patterns exhibited by multiple graphs are captured, thus allowing for partial knowledge transfers between two or more graphs [21, 32]. This task commonly appears in many real-world applications. For instance, the alignment of protein-protein interaction (PPI) networks helps to explore the functionally similar proteins of different species and exhibit their evolutionary relationships [29, 22]. Linking user accounts in different social networks leads to a better understanding of user behavior patterns and thus benefits many downstream tasks, e.g., personalized recommendation [19, 20] and fraud detection [14, 13]. The vision tasks like shape matching and point cloud registration can be formulated as graph matching problems [37, 8].

In practice, achieving exact graph matching is always challenging because of its NP-hardness. Therefore, many methods have been developed to match graphs approximately and efficiently,

---

\*Dixin Luo is the corresponding author. dixin.luo@bit.edu.cn

which can be coarsely categorized into unsupervised methods and semi-supervised ones. Unsupervised graph matching methods often formulate the task as a quadratic assignment problem (QAP) [23] based on the adjacency matrices [35, 17, 48] or other relational matrices [53, 11, 47, 42] of graphs and develop approximate optimization algorithms to solve the problem. Recently, some learning-based methods have been proposed [12, 34, 9], which embed graph nodes and then match the node embeddings across different graphs. To mitigate the NP-hardness, semi-supervised graph matching methods [50, 43, 52, 49] leverage the correspondence between partial nodes as the prior of the matching task and infer the correspondence of the remaining nodes. However, most existing methods merely apply the specific graph information of a single modality (among adjacency matrices, node attributes, and subgraph structures<sup>1</sup>) and thus often leads to non-robust matching results. Although some attempts are made to match graphs based on multi-modal information, e.g., FGW [36], GWL [42], and SLOAlign [33], these methods apply an over-simplified mechanism to fuse the multi-modal information linearly and thus result in sub-optimal performance. Few of them consider fully leveraging all the above information, let alone studying the impacts of the cross-modal information on the matching results.

To overcome the above problem and fill in the blank, in this study we consider the multi-modal information of graphs and their interactions in graph matching tasks, proposing a robust graph matching method, called DHOT-GM, based on a differentiable hierarchical optimal transport framework. As illustrated in Figure 1, our DHOT method formulates the graph matching task as a hierarchical optimal transport problem, leading to a bi-level optimization problem. In particular, given two graphs, we first capture their multi-modal information by a set of relational matrices, which correspond to the adjacency matrices and the inner products of node embedding matrices. In the lower level, we enumerate all pairs of the relational matrices and measure the discrepancies between them by computing the Gromov-Wasserstein (GW) distance [25]. The optimal transport (OT) matrices associated with the GW distances indicate the graph matching results achieved based on the relational matrix pairs within the same modality and across different modalities. Given these lower-level OT matrices, we consider their fusion mechanism in the upper level, learning their weights by solving an OT problem defined for modalities. The significance of the modalities corresponds to the marginal distribution associated with the upper-level OT problem, which can be learned jointly with the weights by the Sinkhorn-scaling algorithm [5]. Solving the two-level optimal transport problems iteratively leads to the proposed DHOT framework. As a result, the weighted sum of the lower-level optimal transport matrices indicates the final graph matching result.

Different from existing graph matching methods, our DHOT-GM method explicitly considers the matching results across different modalities and demonstrates their contributions to improving final matching performance. Additionally, by learning the significance of the modalities and the weights of the modality pairs, our DHOT-GM method can find useful modalities and rely more on their matching results. We test our DHOT-GM method in both synthetic and real-world graph matching tasks and compare it with state-of-the-art unsupervised and semi-supervised graph matching methods. Experimental results demonstrate the superiority of our method and its robustness in highly noisy cases.

---

<sup>1</sup>In this study, we treat adjacency matrices, node attributes, and subgraph structures as three different “modalities”, which reflect different information hidden in graphs.

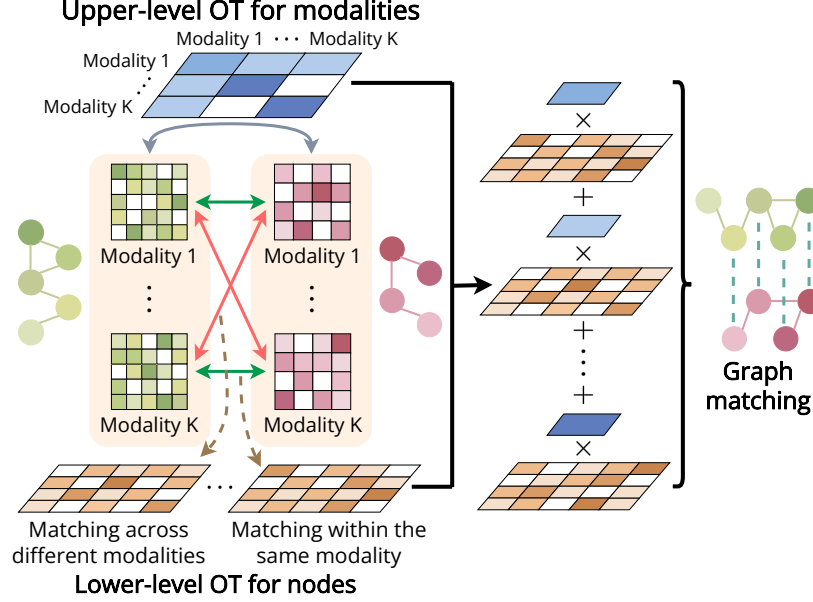


Figure 1: The scheme of DHOT-GM. Given two graphs, we extract a set of relational matrices for each of them based on the information of different modalities. Our method not only matches their relational matrices within the same modality (indicated by the green arrows) but also matches those across different modalities (indicated by the red arrows). Each matching step leads to a lower-level OT matrix for graph nodes, whose weight is determined by an upper-level OT matrix for the modalities. The final matching result is the weighted sum of the lower-level OT matrices.

## 2 Related work

### 2.1 Graph Matching

The most classic solution for graph matching is the QAP-based unsupervised method, which has been widely studied in research [23]. This type of method utilizes various relational matrices of graphs, such as the adjacency matrix of the graph [35, 17, 48], the similarity matrix of node attributes [53, 2, 47], or their fusion matrix [11, 42]. However, due to the NP-hardness of the problem, the QAP-based methods often have high computational complexity, and their graph matching results often suffer from the identifiability issue. In recent years, node embedding-based methods have emerged in unsupervised graph matching. Representative work includes the matrix factorization-based [12] and graph neural network-based methods [34, 9]. They all follow the paradigm of extracting node embeddings first, and then performing graph matching based on the similarity between embeddings.

Semi-supervised graph matching introduces the prior node correspondence to guide the learning process. Typical methods include spectral-based [29], matrix factorization-based [50], and random walk-based [54, 7] methods. In general, the effectiveness of the semi-supervised methods is largely determined by the number of predefined node pairs, while it is often expensive to label matched nodes across different graphs, especially when dealing with real-world graphs that have hundreds and thousands of nodes.

## 2.2 Graph Optimal Transport

Optimal transport (OT) distance and its variants provide an effective metric for probability measures (e.g., distributions). In particular, the OT distance in the Kantorovich form is called Wasserstein distance [15], which corresponds to computing an optimal transport plan (or equivalently, called coupling) between two probability measures. Given the samples of two probability measures, the optimal transport plan between them is formulated as a matrix indicating the pairwise coherency of the samples [31, 25]. Because of this excellent property, OT has received great attention in extensive matching tasks, such as shape matching [30], generative modeling [10], and image-text alignment [3]. In graph data analysis, OT is also gradually being adopted for graph-to-graph comparisons. One of the representatives is the Gromov-Wasserstein (GW) distance that shows excellent performance in graph partitioning [41], graph clustering [40] and graph dictionary learning [38].

Focusing on graph matching, the GW distance can be seen as a relaxation strategy for the QAP problem. Therefore, based on the GW distance, a series of OT-based graph matching methods have been proposed and achieved encouraging performance. For example, GWL [42] is the first OT-based method that jointly learns the node embeddings and finds the node correspondence between two graphs via GW distance. FGW [36] extends the GW distance so that it can be applied to the task of matching attribute graphs. SLOAlign [33] combines GW distance with multi-view structure learning to enhance graph representation power and reduce the effect of structure and feature inconsistency inherited across graphs.

Recently, hierarchical optimal transport (HOT) [28, 1], as a generalization of original OT, is proposed to compare the distributions with structural information, e.g., measuring the distance between different Gaussian mixture models [4]. By solving OT plans at different levels, HOT has achieved encouraging performance in multi-modal distribution [18, 46], multi-modal learning [24], and neural architecture search [44]. However, to the best of our knowledge, this technique has not yet been attempted in the graph matching task.

## 3 Proposed DHOT-GM Method

### 3.1 Motivation

In this study, we denote a graph as  $\mathcal{G} = (\mathcal{V}, \mathbf{A}, \mathbf{X})$ . Here,  $\mathcal{V}$  is the set of nodes.  $\mathbf{A} \in \{0, 1\}^{|\mathcal{V}| \times |\mathcal{V}|}$  is the adjacency matrix, where  $A_{ij} = 1$  denotes the presence of an edge between nodes  $i$  and  $j$ , and  $A_{ij} = 0$  indicates the absence of an edge.  $\mathbf{X} \in \mathbb{R}^{|\mathcal{V}| \times d}$  denotes the node attribute matrix, where  $|\mathcal{V}|$  represents the number of nodes, and each node has a  $d$ -dimensional attribute vector. Given two graphs, i.e.,  $\mathcal{G}_s = (\mathcal{V}_s, \mathbf{A}_s, \mathbf{X}_s)$  and  $\mathcal{G}_t = (\mathcal{V}_t, \mathbf{A}_t, \mathbf{X}_t)$ , graph matching aims to find the correspondence between their nodes. Without the loss of generality, in the following content, we assume that  $|\mathcal{V}_s| \leq |\mathcal{V}_t|$ .

To achieve this aim, we need to find a matrix  $\mathbf{T}^* = [T_{ij}^*] \in \mathbb{R}^{|\mathcal{V}_s| \times |\mathcal{V}_t|}$  indicating the correspondence: for each  $i \in \mathcal{V}_s$ , we can infer its correspondence in  $\mathcal{V}_t$  by  $j^* = \arg \max_{j \in \mathcal{V}_t} T_{ij}^*$ . The inference of  $\mathbf{T}^*$  is often formulated in a QAP format [23], i.e.,

$$\mathbf{T}^* = \arg \max_{\mathbf{T} \in \Omega} \langle \mathbf{D}_s \mathbf{T} \mathbf{D}_t^\top, \mathbf{T} \rangle, \quad (1)$$

where  $\langle \cdot, \cdot \rangle$  represents the inner product of matrix,  $\Omega$  is the feasible domain of  $\mathbf{T}$ , and  $\{\mathbf{D}_s = [D_{ij}^s] \in \mathbb{R}^{|\mathcal{V}_s| \times |\mathcal{V}_s|}, \mathbf{D}_t = [D_{ij}^t] \in \mathbb{R}^{|\mathcal{V}_t| \times |\mathcal{V}_t|}\}$  are two relational matrices extracted from the graphs.

In the classic QAP problem, the feasible domain  $\Omega = \{\mathbf{T} \in \{0, 1\}^{|\mathcal{V}_s| \times |\mathcal{V}_t|} | \mathbf{T} \mathbf{1}_{|\mathcal{V}_t|} = \mathbf{1}_{|\mathcal{V}_s|}, \mathbf{T}^\top \mathbf{1}_{|\mathcal{V}_s|} \leq \mathbf{1}_{|\mathcal{V}_t|}\}$ , leading to a combinatorial optimization problem. To simplify the computation, we often relax the feasible domain to a set of doubly-stochastic matrices, i.e.,  $\Omega(\boldsymbol{\mu}_s, \boldsymbol{\mu}_t) = \{\mathbf{T} > \mathbf{0}_{|\mathcal{V}_s| \times |\mathcal{V}_t|} | \mathbf{T} \mathbf{1}_{|\mathcal{V}_t|} =$

$\boldsymbol{\mu}_s, \mathbf{T}^\top \mathbf{1}_{|\mathcal{V}_s|} = \boldsymbol{\mu}_t\}$ , where  $\boldsymbol{\mu}_s$  and  $\boldsymbol{\mu}_t$  are two vectors defined on  $(|\mathcal{V}_s| - 1)$ -Simplex and  $(|\mathcal{V}_t| - 1)$ -Simplex, respectively. Typically, we can set  $\boldsymbol{\mu}_s = \frac{1}{|\mathcal{V}_s|} \mathbf{1}_{|\mathcal{V}_s|}$  and  $\boldsymbol{\mu}_t = \frac{1}{|\mathcal{V}_t|} \mathbf{1}_{|\mathcal{V}_t|}$  when there is no prior knowledge [42]. In such a situation, equation 1 is equivalent to the computational problem of the Gromov-Wasserstein discrepancy between  $\mathbf{D}_s$  and  $\mathbf{D}_t$  [26], i.e.,

$$\begin{aligned} d_{GW}(\mathbf{D}_s, \mathbf{D}_t) &:= \min_{\mathbf{T} \in \Omega(\boldsymbol{\mu}_s, \boldsymbol{\mu}_t)} \sum_{i,j,k,l} |D_{ij}^s - D_{kl}^t|^2 T_{ij} T_{kl} \\ &= \min_{\mathbf{T} \in \Omega(\boldsymbol{\mu}_s, \boldsymbol{\mu}_t)} \langle \mathbf{L}(\mathbf{D}_s, \mathbf{D}_t, \mathbf{T}), \mathbf{T} \rangle, \end{aligned} \quad (2)$$

where  $\mathbf{L}(\mathbf{D}_s, \mathbf{D}_t, \mathbf{T}) = (\mathbf{D}_s \odot \mathbf{D}_s) \boldsymbol{\mu}_s \mathbf{1}_{|\mathcal{V}_t|}^\top + \mathbf{1}_{|\mathcal{V}_s|} \boldsymbol{\mu}_t^\top (\mathbf{D}_t \odot \mathbf{D}_t)^\top - 2\mathbf{D}_s \mathbf{T} \mathbf{D}_t^\top$  and  $\odot$  denotes the Hadamard product of matrix. The optimal solution of equation 2, i.e.,  $\mathbf{T}^*$ , is called the optimal transport matrix, which can be explained as the joint distribution of the nodes. In particular, its element  $T_{ij}^*$  is the coherency probability of the node  $i \in \mathcal{V}_s$  and the node  $j \in \mathcal{V}_t$ .

Typically, each relational matrix records the pairwise relations or similarities for the nodes of a graph, which can be implemented as the adjacency matrix of the graph [17, 35, 48], the similarity matrix of node attributes [53, 2, 47], or their fusion matrix [11, 42, 36, 33]. However, in our opinion, existing methods do not fully leverage the above information and thus suffer from the following two issues.

- **Non-robust matching based on a single relational matrix pair.** As aforementioned, many methods match graphs based on their relational matrices in a single modality. For example, the work in [41, 17, 35, 48] sets the  $\mathbf{D}_s$  and  $\mathbf{D}_t$  in equation 2 as the adjacency matrices. However, merely applying a single relational matrix pair often leads to non-robust matching results, especially in highly-noisy cases.
- **Ignoring the potential of cross-modal matching.** Recently, some work considers fusing multi-modal relational matrices [11, 36]. For example, the GWL in [42] and the SLOAlign method in [33] construct the  $\mathbf{D}_s$  and  $\mathbf{D}_t$  in equation 2 by a linear fusion mechanism:

$$\mathbf{D}_s = \sum_{k=1}^K \alpha_k \mathbf{D}_s^{(k)}, \quad \mathbf{D}_t = \sum_{k=1}^K \alpha_k \mathbf{D}_t^{(k)}. \quad (3)$$

Here,  $K$  modalities are considered, and  $\{\mathbf{D}_s^{(k)}, \mathbf{D}_t^{(k)}\}$  is the relational matrix pair corresponding to the  $k$ -th modality. The coefficients  $\{\alpha_k\}_{k=1}^K$  control the significance of the modalities, which can be fixed [42] or learnable [33]. Although the fused relational matrices help to improve the robustness of graph matching, the linear fusion mechanism is often over-simplified — the fusion step itself results in the loss of structural information.<sup>2</sup> Moreover, existing methods require the relational matrices of different graphs to be constructed in the same manner. For the relational matrices in different modalities, existing methods neither consider their matching problems nor study their potential impacts on the graph matching results, which may result in sub-optimal performance.

In the following content, we will propose a robust graph matching method, resolving the above two issues in a differentiable hierarchical optimal transport framework.

### 3.2 A Differentiable Hierarchical Optimal Transport Framework

Instead of using a single relational matrix pair or fusing multi-modal relational matrices linearly, our method extracts multi-modal relational matrices and treats them as a set. As a result, a graph

---

<sup>2</sup>For example, merely based on the fused matrix  $\mathbf{D}_s$ , we cannot obtain its multi-modal components  $\{\mathbf{D}_s^{(k)}\}_{k=1}^K$ . The fusion step eliminates the identifiability of different modalities.

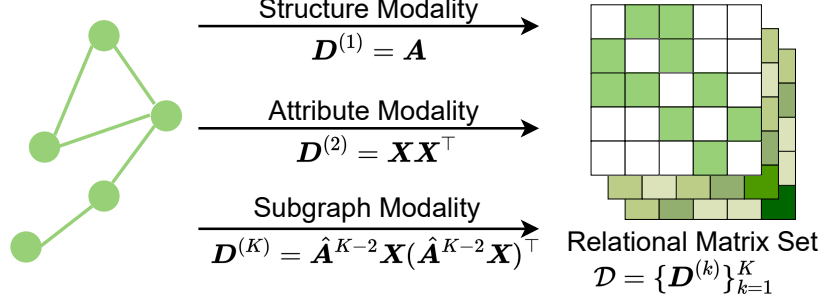


Figure 2: The pipeline for extracting relational matrices.

can be represented as  $\mathcal{G} = (\mathcal{V}, \mathcal{D})$ , where  $\mathcal{D} = \{\mathbf{D}^{(k)} \in \mathbb{R}^{|\mathcal{V}| \times |\mathcal{V}|}\}_{k=1}^K$  is the set of  $K$  modalities' relational matrices and  $K$  is the number of modalities. As shown in Figure 2, we extract the  $K$  relational matrices from the following three resources.

- **Graph Topology.** The adjacency matrix of a graph captures its topological information, which can be treated as a relational matrix in nature, i.e.,  $\mathbf{D}^{(1)} = \mathbf{A}$ .
- **Node Attributes.** The node attributes are the information imposed on graph nodes, and the inner product between arbitrary two nodes encodes their pairwise similarity. Therefore, given normalized node attribute matrix  $\mathbf{X} = [\mathbf{x}_1, \dots, \mathbf{x}_{|\mathcal{V}|}]^\top \in \mathbb{R}^{|\mathcal{V}| \times d}$ , we construct the second relational matrix as  $\mathbf{D}^{(2)} = \mathbf{X}\mathbf{X}^\top$ .
- **Subgraph Structures.** Both the adjacency matrix and the node attribute similarity matrix can only capture the relationships of node pairs. To capture the relationships of subgraph pairs, we need a message-passing mechanism to encode the neighborhood information of each node. In this study, we apply a  $N$ -layer parameter-free message-passing [16] as follows:  $\mathbf{Z}^{(0)} = \mathbf{X}$ , and

$$\mathbf{Z}^{(n)} = (\mathbf{M}^{-\frac{1}{2}} \hat{\mathbf{A}} \mathbf{M}^{-\frac{1}{2}}) \mathbf{Z}^{(n-1)}, \text{ for } n = 1, \dots, N, \quad (4)$$

where  $\hat{\mathbf{A}} = \mathbf{A} + \mathbf{I}$  is the adjacency matrix with self-loop and  $\mathbf{I}$  is the identity matrix,  $\mathbf{M}$  is the degree matrix of  $\hat{\mathbf{A}}$  that  $M_{ii} = \sum_j \hat{A}_{ij}$ . Obviously,  $\mathbf{Z}^{(n)} = [\mathbf{z}_1^{(n)}, \dots, \mathbf{z}_{|\mathcal{V}|}^{(n)}]^\top \in \mathbb{R}^{|\mathcal{V}| \times d}$  is the output after  $n$ -step message-passing, and  $\mathbf{z}_i^{(n)}$  encodes the subgraph corresponding to the  $n$ -hop neighborhood of the node  $i$ . Accordingly, we can construct multiple relational matrices by the inner products of the embeddings generated by different layers, i.e.,  $\mathbf{D}^{(n+2)} = \mathbf{Z}^{(n)} \mathbf{Z}^{(n)\top}$  for  $n = 1, \dots, N$ , where  $\mathbf{D}^{(n+2)}$  indicates the pairwise similarities of the  $n$ -hop subgraphs. From the viewpoint of graph spectral filtering [6], the message-passing steps in equation 4 are equivalent to applying a low-pass graph filter to  $\mathbf{X}$ .

Setting the number of layers to  $N = K - 2$ , we derive the multi-modal relational matrix set  $\mathcal{D} = \{\mathbf{D}^{(k)}\}_{k=1}^K$  by

$$\mathbf{D}^{(1)} = \mathbf{A}, \mathbf{D}^{(2)} = \mathbf{X}\mathbf{X}^\top, \mathbf{D}^{(k)} = \mathbf{Z}^{(k-2)} \mathbf{Z}^{(k-2)\top}, 2 < k \leq K. \quad (5)$$

Given two graphs, i.e.,  $\mathcal{G}_s(\mathcal{V}_s, \mathcal{D}_s)$  and  $\mathcal{G}_t(\mathcal{V}_t, \mathcal{D}_t)$ , where  $\mathcal{D}_s$  and  $\mathcal{D}_t$  are constructed by equation 5, our method formulates the graph matching task in the following differentiable hierarchical optimal transport framework. In particular, we first define the hierarchical optimal transport distance between the two graphs, denoted as

$$d_{HOT}(\mathcal{G}_s, \mathcal{G}_t) := d_W(\boldsymbol{\nu}_s, \boldsymbol{\nu}_t; \mathbf{D}_{GW}(\mathcal{D}_s, \mathcal{D}_t)), \quad (6)$$

which corresponds to the composition of OT problems in two levels.

### 3.2.1 Lower-level Optimal Transports for Nodes

The  $\mathbf{D}_{GW}(\mathcal{D}_s, \mathcal{D}_t)$  in equation 6 is a Gromov-Wasserstein distance matrix with size  $K \times K$ , i.e.,  $\mathbf{D}_{GW}(\mathcal{D}_s, \mathcal{D}_t) = [d_{GW}(\mathbf{D}_s^{(p)}, \mathbf{D}_t^{(q)})] \in \mathbb{R}^{K \times K}$ . Here, the element  $d_{GW}(\mathbf{D}_s^{(p)}, \mathbf{D}_t^{(q)})$  corresponds to the GW distance between the  $p$ -th relational matrix of  $\mathcal{G}_s$  and the  $q$ -th relational matrix of  $\mathcal{G}_t$ . As the definition in equation 2, the computation of  $d_{GW}(\mathbf{D}_s^{(p)}, \mathbf{D}_t^{(q)})$  corresponds to solving a constrained nonsmooth nonconvex optimization problem. Its optimal solution, denoted as  $\mathbf{T}^{(p,q)}$ , is the optimal transport matrix indicating the graph matching result derived based on  $\mathbf{D}_s^{(p)}$  and  $\mathbf{D}_t^{(q)}$ .

- **Remark 1.** Enumerating all relational matrix pairs, our method computes  $K^2$  GW distances and derives the GW distance matrix  $\mathbf{D}_{GW}$  associated with a set of optimal transport matrices, denoted as  $\mathcal{T} = \{\mathbf{T}^{(p,q)}\}_{p=1,q=1}^K$ . When  $p = q$ ,  $\mathbf{T}^{(p,q)}$  captures the node correspondence between  $\mathcal{G}_s$  and  $\mathcal{G}_t$  based on the relational information within the same modality. When  $p \neq q$ ,  $\mathbf{T}^{(p,q)}$  captures the node correspondence between  $\mathcal{G}_s$  and  $\mathcal{G}_t$  across different modalities. In other words, different from existing graph matching methods, our method explicitly considers matching the graphs based on their cross-modal similarities, as we claimed in the Introduction.

### 3.2.2 An Upper-level Optimal Transport for Modalities

Taking the GW distance matrix  $\mathbf{D}_{GW}$  as the grounding cost, we further compute the Wasserstein distance between the modalities' distributions, i.e., the  $d_W(\boldsymbol{\nu}_s, \boldsymbol{\nu}_t; \mathbf{D}_{GW})$  in equation 6. In particular, its definition is shown below:

$$\begin{aligned} d_W(\boldsymbol{\nu}_s, \boldsymbol{\nu}_t; \mathbf{D}_{GW}) &:= \min_{\boldsymbol{\Theta} \in \Omega(\boldsymbol{\nu}_s, \boldsymbol{\nu}_t)} \sum_{p=1}^K \sum_{q=1}^K d_{GW}(\mathbf{D}_s^{(p)}, \mathbf{D}_t^{(q)}) \theta_{pq} \\ &= \min_{\boldsymbol{\Theta} \in \Omega(\boldsymbol{\nu}_s, \boldsymbol{\nu}_t)} \langle \mathbf{D}_{GW}, \boldsymbol{\Theta} \rangle. \end{aligned} \quad (7)$$

Here,  $\boldsymbol{\nu}_s, \boldsymbol{\nu}_t$  are two vectors in the  $(K-1)$ -Simplex, indicating the significance of the  $K$  modalities for  $\mathcal{G}_s$  and  $\mathcal{G}_t$ , respectively.  $\Omega(\boldsymbol{\nu}_s, \boldsymbol{\nu}_t)$  is the set of the doubly-stochastic matrices that take  $\boldsymbol{\nu}_s$  and  $\boldsymbol{\nu}_t$  as marginals.  $\boldsymbol{\Theta} = [\theta_{pq}] \in \Pi(\boldsymbol{\nu}_s, \boldsymbol{\nu}_t)$  is the transport matrix defined for the modalities. It can be explained as a joint distribution of the modalities corresponding to different graphs. In particular, its element  $\theta_{pq}$  can be explained as the coherency probability of the  $p$ -th modality of  $\mathcal{G}_s$  and the  $q$ -th modality of  $\mathcal{G}_t$ .

- **Remark 2.** In principle, the matrix  $\boldsymbol{\Theta}$  indicates the significance of different modality pairs. In particular, when the coherency probability of the modality pair  $(p, q)$  (i.e.,  $\theta_{pq}$ ) is large, the corresponding GW distance  $d_{GW}(\mathbf{D}_s^{(p)}, \mathbf{D}_t^{(q)})$  should be small, which means that  $\mathbf{D}_s^{(p)}$  and  $\mathbf{D}_t^{(q)}$  are matched well and their matching result  $\mathbf{T}^{(p,q)}$  is significant.

### 3.2.3 Robust Graph Matching by Minimizing HOT

The composition of the above two-level optimal transport problems leads to the HOT distance shown in equation 6. The principle of our DHOT-GM method is matching graphs by minimizing the HOT distance between them with learnable and regularized modality distributions, i.e.,

$$\mathcal{T}, \boldsymbol{\Theta}, \boldsymbol{\nu}_t, \boldsymbol{\nu}_s = \arg \min_{\mathcal{T}, \boldsymbol{\Theta}, \boldsymbol{\nu}_t, \boldsymbol{\nu}_s} \underbrace{d_W(\boldsymbol{\nu}_s, \boldsymbol{\nu}_t; \mathbf{D}_{GW})}_{d_{HOT}(\mathcal{G}_s, \mathcal{G}_t)} + \underbrace{\left( KL(\boldsymbol{\nu}_s \| \frac{1}{K} \mathbf{1}_K) + KL(\boldsymbol{\nu}_t \| \frac{1}{K} \mathbf{1}_K) \right)}_{\text{Regularizer of modality significance}}. \quad (8)$$

Here, the first term is the HOT distance between the two graphs. It corresponds to the computation of the  $K^2$  lower-level optimal transport matrices  $\mathcal{T} = \{\mathbf{T}^{(p,q)}\}_{p,q=1}^K$  and the upper-level optimal transport matrix  $\Theta$ . Note that, we call this optimization problem ‘‘Differentiable Hierarchical Optimal Transport’’ because the marginals  $\nu_s$  and  $\nu_t$  are learnable variables in the problem. The second term in equation 8 includes the regularizers of the marginals. Each regularizer is implemented as the KL-divergence between a marginal and its uniform prior, which helps to avoid trivial solutions (e.g.,  $\nu_s$  and  $\nu_t$  are one-hot vectors and thus only one modality pair is used to match graphs).

Given  $\mathcal{T}$  and  $\Theta$ , we compute the final matching result as the weighted sum of all  $\mathbf{T}^{(p,q)}$ ’s, i.e.,

$$\mathbf{T} = \sum_{p=1}^K \sum_{q=1}^K \theta_{pq} \mathbf{T}^{(p,q)}. \quad (9)$$

Accordingly, the final matching result is dominated by the  $\mathbf{T}^{(p,q)}$ ’s corresponding to the significant modality pairs.

### 3.3 Connections to Existing Methods

The DHOT framework allows us to explicitly capture the cross-modal matching results (i.e.,  $\{\mathbf{T}^{(p,q)}\}_{p \neq q}$ ). We reveal the connections of our DHOT-GM method to existing methods as follows.

#### 3.3.1 Connection to single-modal graph matching

As aforementioned, when solving equation 8 without the regularizer, we have the trivial solution

$$\min_{\mathcal{T}, \Theta, \nu_t, \nu_s} d_W(\nu_s, \nu_t; \mathbf{D}_{GW}) = \min_{p,q \in \{1, \dots, K\}} d_{GW}(\mathbf{D}_s^{(p)}, \mathbf{D}_t^{(q)}), \quad (10)$$

in which the optimal  $\nu_t^*$  and  $\nu_s^*$  are one-hot vectors, and their non-zero elements indicate the modality pair  $(p, q)$  that corresponds to the minimum GW distance. When  $p = q$ , this trivial solution corresponds to matching  $\mathcal{G}_s$  and  $\mathcal{G}_t$  based on the relational matrices within the same modality. In such a situation, DHOT-GM degrades to the classic single-modal graph matching strategy [41, 17, 35, 48].

#### 3.3.2 Connection to linear fusion-based multi-modal graph matching

The GWL [42] and SLOAlign [33] compute  $d_{GW} \left( \sum_{k=1}^K \mathbf{D}_s^{(k)}, \sum_{k=1}^K \mathbf{D}_t^{(k)} \right)$ , leading to a  $\mathbf{T}^*$  shared by all modality pairs. Accordingly, we denote

$$\mathbf{T}^* = \arg \min_{\mathbf{T}} d_{GW} \left( \sum_{k=1}^K \mathbf{D}_s^{(k)}, \sum_{k=1}^K \mathbf{D}_t^{(k)} \right) = \arg \min_{\mathbf{T}} \left\langle \mathbf{L} \left( \sum_{k=1}^K \mathbf{D}_s^{(k)}, \sum_{k=1}^K \mathbf{D}_t^{(k)}, \mathbf{T} \right), \mathbf{T} \right\rangle. \quad (11)$$

Assume that  $\Theta = [\frac{1}{K^2}]$  is fixed as a uniform distribution. In such a situation, we can find that the DHOT loss function of our method degrades to  $\frac{1}{K^2} \sum_{p,q=1}^K d_{GW}(\mathbf{D}_s^{(p)}, \mathbf{D}_t^{(q)})$ , and it has an upper bound  $\frac{1}{K^2} d_{GW} \left( \sum_{p=1}^K \mathbf{D}_s^{(p)}, \sum_{q=1}^K \mathbf{D}_t^{(q)} \right) + C$ , where  $C > 0$  is a positive constant independent of



$\mathbf{T}^*$ . The proof is given as follows.

$$\begin{aligned}
\frac{1}{K^2} \sum_{p,q=1}^K d_{GW}(\mathbf{D}_s^{(p)}, \mathbf{D}_t^{(q)}) &\leq \frac{1}{K^2} \sum_{p,q=1}^K \left\langle \mathbf{L}(\mathbf{D}_s^{(p)}, \mathbf{D}_t^{(q)}, \mathbf{T}^*), \mathbf{T}^* \right\rangle \\
&= \frac{1}{K^2} \sum_{p,q=1}^K \left\langle (\mathbf{D}_s^{(p)} \odot \mathbf{D}_s^{(p)}) \boldsymbol{\nu}_s \mathbf{1}^\top + \mathbf{1} \boldsymbol{\nu}_t^\top (\mathbf{D}_t^{(q)} \odot \mathbf{D}_t^{(q)}) - 2\mathbf{D}_s^{(p)} \mathbf{T}^* \mathbf{D}_t^{(q)}, \mathbf{T}^* \right\rangle \\
&= \frac{1}{K^2} \sum_{p,q=1}^K \left\langle (\mathbf{D}_s^{(p)} \odot \mathbf{D}_s^{(p)}) \boldsymbol{\nu}_s \mathbf{1}^\top + \mathbf{1} \boldsymbol{\nu}_t^\top (\mathbf{D}_t^{(q)} \odot \mathbf{D}_t^{(q)}), \mathbf{T}^* \right\rangle - \frac{2}{K^2} \left\langle \left( \sum_{p=1}^K \mathbf{D}_s^{(p)} \right) \mathbf{T}^* \left( \sum_{q=1}^K \mathbf{D}_t^{(q)} \right), \mathbf{T}^* \right\rangle \\
&= \frac{1}{K^2} \sum_{p,q=1}^K \left\langle (\mathbf{D}_s^{(p)} \odot \mathbf{D}_s^{(p)}) \boldsymbol{\nu}_s \mathbf{1}^\top + \mathbf{1} \boldsymbol{\nu}_t^\top (\mathbf{D}_t^{(q)} \odot \mathbf{D}_t^{(q)}), \mathbf{T}^* \right\rangle + \frac{1}{K^2} d_{GW} \left( \sum_{p=1}^K \mathbf{D}_s^{(p)}, \sum_{q=1}^K \mathbf{D}_t^{(q)} \right) \\
&\quad - \frac{1}{K^2} \left\langle \left( \sum_{p=1}^K \mathbf{D}_s^{(p)} \odot \sum_{p=1}^K \mathbf{D}_s^{(p)} \right) \boldsymbol{\nu}_s \mathbf{1}^\top + \mathbf{1} \boldsymbol{\nu}_t^\top \left( \sum_{q=1}^K \mathbf{D}_t^{(q)} \odot \sum_{q=1}^K \mathbf{D}_t^{(q)} \right), \mathbf{T}^* \right\rangle \\
&= \frac{1}{K^2} d_{GW} \left( \sum_{p=1}^K \mathbf{D}_s^{(p)}, \sum_{q=1}^K \mathbf{D}_t^{(q)} \right) + \frac{1}{K^2} \text{tr} \left[ \left( K \sum_{p=1}^K (\mathbf{D}_s^{(p)} \odot \mathbf{D}_s^{(p)}) - \left( \sum_{p=1}^K \mathbf{D}_s^{(p)} \odot \sum_{p=1}^K \mathbf{D}_s^{(p)} \right) \right) \boldsymbol{\nu}_s \boldsymbol{\nu}_t^\top \right] \\
&\quad + \frac{1}{K^2} \text{tr} \left[ \boldsymbol{\nu}_s \boldsymbol{\nu}_t^\top \left( K \sum_{p=1}^K (\mathbf{D}_t^{(q)} \odot \mathbf{D}_t^{(q)}) - \left( \sum_{q=1}^K \mathbf{D}_t^{(q)} \odot \sum_{q=1}^K \mathbf{D}_t^{(q)} \right) \right) \right] \\
&= \frac{1}{K^2} d_{GW} \left( \sum_{p=1}^K \mathbf{D}_s^{(p)}, \sum_{q=1}^K \mathbf{D}_t^{(q)} \right) + C.
\end{aligned} \tag{12}$$

Additionally, we can further prove that when  $\Theta = [\frac{1}{K^2}]$ , there exists a lower bound for  $d_W(\boldsymbol{\nu}_s, \boldsymbol{\nu}_t; \mathbf{D}_{GW})$ , i.e.,

$$\begin{aligned}
d_{GW} \left( \sum_{p=1}^K \mathbf{D}_s^{(p)}, \sum_{q=1}^K \mathbf{D}_t^{(q)} \right) &= \text{tr} \left[ \left( \sum_{p=1}^K \mathbf{D}_s^{(p)} \odot \sum_{p=1}^K \mathbf{D}_s^{(p)} \right) \boldsymbol{\nu}_s \boldsymbol{\nu}_t^\top + \boldsymbol{\nu}_s \boldsymbol{\nu}_t^\top \left( \sum_{q=1}^K \mathbf{D}_t^{(q)} \odot \sum_{q=1}^K \mathbf{D}_t^{(q)} \right) \right] - \\
&\quad 2 \left\langle \left( \sum_{p=1}^K \mathbf{D}_s^{(p)} \right) \mathbf{T}^* \left( \sum_{q=1}^K \mathbf{D}_t^{(q)} \right), \mathbf{T}^* \right\rangle \\
&\leq K \sum_{p=1}^K \text{tr} \left[ \left( \sum_{p=1}^K \mathbf{D}_s^{(p)} \odot \sum_{p=1}^K \mathbf{D}_s^{(p)} \right) \boldsymbol{\nu}_s \boldsymbol{\nu}_t^\top \right] + K \sum_{q=1}^K \text{tr} \left[ \boldsymbol{\nu}_s \boldsymbol{\nu}_t^\top \left( \sum_{q=1}^K \mathbf{D}_t^{(q)} \odot \sum_{q=1}^K \mathbf{D}_t^{(q)} \right) \right] - \\
&\quad 2 \left\langle \left( \sum_{p=1}^K \mathbf{D}_s^{(p)} \right) \mathbf{T}^* \left( \sum_{q=1}^K \mathbf{D}_t^{(q)} \right), \mathbf{T}^* \right\rangle \\
&\leq K \sum_{p=1}^K \text{tr} \left[ \left( \sum_{p=1}^K \mathbf{D}_s^{(p)} \odot \sum_{p=1}^K \mathbf{D}_s^{(p)} \right) \boldsymbol{\nu}_s \boldsymbol{\nu}_t^\top \right] + K \sum_{q=1}^K \text{tr} \left[ \boldsymbol{\nu}_s \boldsymbol{\nu}_t^\top \left( \sum_{q=1}^K \mathbf{D}_t^{(q)} \odot \sum_{q=1}^K \mathbf{D}_t^{(q)} \right) \right] - \\
&\quad 2 \sum_{p,q=1}^K \left\langle \mathbf{D}_s^{(p)} \mathbf{T}^{(p,q)} \mathbf{D}_t^{(q)}, \mathbf{T}^{(p,q)} \right\rangle \\
&= \sum_{p,q=1}^K d_{GW}(\mathbf{D}_s^{(p)}, \mathbf{D}_t^{(q)}).
\end{aligned} \tag{13}$$

---

**Algorithm 1** The computation of  $d_{GW}(\mathbf{D}_s^{(p)}, \mathbf{D}_t^{(q)})$

---

**Require:** Marginals  $\mu_s, \nu_t$ , relational matrix  $\mathbf{D}_s, \mathbf{D}_t$ , matching matrix  $\mathbf{T}$ , entropic regularizer  $\lambda$ , the number of outer/inner iterations  $\{M, N\}$ .

```

1: Initialize  $\mathbf{b} = \mu_t$  and  $\mathbf{T} = \mu_s \mu_t^\top$ 
2: for  $m = 1, \dots, M$  do
3:    $\mathbf{G} = \exp(-L(\mathbf{D}_s^{(p)}, \mathbf{D}_t^{(q)}, \mathbf{T})/\lambda) \odot \mathbf{T}$ 
4:   for  $n = 1, \dots, N$  do
5:      $\mathbf{a} = \mu_s / (\mathbf{G}\mathbf{b})$ , and then  $\mathbf{b} = \mu_t / (\mathbf{G}^\top \mathbf{a})$ 
6:   end for
7:    $\mathbf{T} = \text{diag}(\mathbf{a})\mathbf{G} \text{diag}(\mathbf{b})$ 
8: end for
9:  $d_{GW}(\mathbf{D}_s^{(p)}, \mathbf{D}_t^{(q)}) = \langle L(\mathbf{D}_s^{(p)}, \mathbf{D}_t^{(q)}, \mathbf{T}), \mathbf{T} \rangle$ 
10: return  $d_{GW}(\mathbf{D}_s^{(p)}, \mathbf{D}_t^{(q)})$ , and  $\mathbf{T}^{(p,q)} \leftarrow \mathbf{T}$ .
```

---

Combined with the previous proof, we have

$$\frac{1}{K^2} d_{GW}\left(\sum_{p=1}^K \mathbf{D}_s^{(p)}, \sum_{q=1}^K \mathbf{D}_t^{(q)}\right) \leq \frac{1}{K^2} \sum_{p,q=1}^K d_{GW}(\mathbf{D}_s^{(p)}, \mathbf{D}_t^{(q)}) \leq \frac{1}{K^2} d_{GW}\left(\sum_{p=1}^K \mathbf{D}_s^{(p)}, \sum_{q=1}^K \mathbf{D}_t^{(q)}\right) + C. \quad (14)$$

Therefore, DHOT-GM and GW distance (SLOTAlign) are equivalent when  $\Theta$  is a uniform distribution. Applying learnable  $\Theta$  makes DHOT-GM distinguished from existing methods.

### 3.4 Optimization Algorithm

We propose a bi-level learning algorithm to solve the DHOT problem in equation 8. In the lower-level, we need to compute  $K^2$  GW distances. In this study, we apply the proximal gradient algorithm [41] to compute each GW distance efficiently. In theory, the algorithm ensures that the variables converge to a stationary point [42]. The algorithmic scheme is shown in Algorithm 1. For a graph with  $V$  nodes and  $K$  modalities, the computational complexity of this algorithm is  $\mathcal{O}(K^2 V^3)$  and can be reduced to  $\mathcal{O}(K^2 V^2 d)$  when considering the low-rank structure of relational matrices [27].

In the upper-level, we need to *i*) compute a Wasserstein distance with  $K \times K$  size and *ii*) update the marginals. We can achieve these two steps jointly in an algorithmic framework based on the Sinkhorn-scaling algorithm [5]. Specifically, we rewrite the upper-level problem in equation 7 by introducing an entropic regularizer, i.e.,

$$\min_{\Theta \in \Omega(\nu_s, \nu_t)} \langle \mathbf{D}_{GW}, \Theta \rangle + \lambda H(\Theta), \quad (15)$$

where  $H(\Theta) = \langle \Theta, \log \Theta \rangle$ , and  $\lambda$  is the hyperparameter controlling the importance of the entropy term.

This entropic regularizer improves the smoothness of the original problem. Accordingly, the entropic OT problem in equation 15 can be solved efficiently by the Sinkhorn-scaling algorithm [5], as shown in Algorithm 2, whose computational complexity is  $\mathcal{O}(K^2)$ .

When updating the marginals, we apply the gradient descent algorithm, i.e.,

$$\nu_s \leftarrow \nu_s - \gamma \frac{\partial d_w(\nu_s, \nu_t)}{\partial \nu_s}, \quad \nu_t \leftarrow \nu_t - \gamma \frac{\partial d_w(\nu_s, \nu_t)}{\partial \nu_t}, \quad (16)$$

---

**Algorithm 2** Compute  $d_W(\boldsymbol{\nu}_s, \boldsymbol{\nu}_t; \mathbf{D}_{GW})$  with learnable  $\{\boldsymbol{\nu}_s, \boldsymbol{\nu}_t\}$

---

**Require:** Marginals  $\boldsymbol{\nu}_s, \boldsymbol{\nu}_t$ , cost matrix  $\mathbf{D}_{GW}$ , the number of modalities  $K$ , entropic regularizer  $\lambda$ , learning rate  $\gamma$ , the number of Sinkhorn-Knopp iterations  $M$ , the importance factor matrix  $\Theta$ .

- 1:  $\mathbf{b}^{(0)} = \frac{1}{K} \mathbf{1}_K$ ,  $\Theta = \boldsymbol{\nu}_s \boldsymbol{\nu}_t^\top$ , and  $\mathbf{Q} = \exp(-\mathbf{D}_{GW}/\lambda)$
  - 2: **for**  $m = 1, \dots, M$  **do**
  - 3:    $\mathbf{a}^{(m)} = \boldsymbol{\nu}_s / (\mathbf{Q} \mathbf{b}^{(m-1)})$ , and then  $\mathbf{b}^{(m)} = \boldsymbol{\nu}_t / (\mathbf{Q}^\top \mathbf{a}^{(m-1)})$
  - 4: **end for**
  - 5:  $\boldsymbol{\nu}_s = \boldsymbol{\nu}_s - \gamma(\log \mathbf{a} - \frac{\log \mathbf{a}^\top \mathbf{1}}{\mathbf{Q}} \mathbf{1})/\lambda$ ,  $\boldsymbol{\nu}_t = \boldsymbol{\nu}_t - \gamma(\log \mathbf{b} - \frac{\log \mathbf{b}^\top \mathbf{1}}{\mathbf{Q}} \mathbf{1})/\lambda$
  - 6: **return**  $\Theta \leftarrow \text{diag}(\mathbf{a}^{(M)}) \mathbf{Q} \text{diag}(\mathbf{b}^{(M)})$ ,  $\boldsymbol{\nu}_s$ , and  $\boldsymbol{\nu}_t$ .
- 

**Algorithm 3** DHOT-GM

---

**Require:** Source graph  $\mathcal{G}_s = (\mathcal{V}_s, \mathbf{A}_s, \mathbf{X}_s)$ , target graph  $\mathcal{G}_t = (\mathcal{V}_t, \mathbf{A}_t, \mathbf{X}_t)$ , the number of modalities  $K$ , the number of training iterations  $T$ .

- 1: Reformulate the two graphs as  $\mathcal{G}_s = (\mathcal{V}_s, \mathcal{D}_s)$  and  $\mathcal{G}_t = (\mathcal{V}_t, \mathcal{D}_t)$  according to equation 5.
  - 2:  $\boldsymbol{\nu}_s = \frac{1}{K} \mathbf{1}_K$ ,  $\boldsymbol{\nu}_t = \frac{1}{K} \mathbf{1}_K$ ,  $\boldsymbol{\mu}_s = \frac{1}{|\mathcal{V}_s|} \mathbf{1}_{|\mathcal{V}_s|}$ ,  $\boldsymbol{\mu}_t = \frac{1}{|\mathcal{V}_t|} \mathbf{1}_{|\mathcal{V}_t|}$
  - 3:  $\mathbf{T} = \boldsymbol{\mu}_s \boldsymbol{\mu}_t^\top$
  - 4: **for**  $t = 1, \dots, T$  **do**
  - 5:   **for**  $D_s^{(p)} \in \mathcal{D}_s, D_t^{(q)} \in \mathcal{D}_t$  **do**
  - 6:     Get  $d_{GW}^{(p,q)}(D_s^{(p)}, D_t^{(q)})$  and  $\mathbf{T}^{(p,q)}$  via Algorithm 1.
  - 7:   **end for**
  - 8:   Construct  $\mathcal{T} = \{\mathbf{T}^{(p,q)}\}_{p=1, q=1}^K$  and  $\mathbf{C} = [d_{GW}^{(p,q)}]$ .
  - 9:   Update  $\boldsymbol{\nu}_s, \boldsymbol{\nu}_t$  and  $\Theta$  via Algorithm 2.
  - 10:  $\mathbf{T} = \sum_{p=1}^K \sum_{q=1}^K \theta_{pq} \mathbf{T}^{(p,q)}$ .
  - 11: **end for**
- 

where  $\gamma$  is the learning rate. The computation of the gradients can be efficiently approximated associated with the Sinkhorn-scaling iterations [39, 24], as shown in Line 5 of Algorithm 2.

In summary, our DHOT-GM method first computes  $K^2$  GW distances and derives the corresponding optimal transport matrices, each of which indicates a matching result for graph nodes. Then, the significance of the matrices is computed by solving an entropic OT problem with learnable marginals. The final matching result is obtained by aggregating all the matching matrices according to equation 9. Algorithm 3 gives the pipeline of our method.

## 4 Experiments

### 4.1 Experimental Setup

#### 4.1.1 Baselines

To demonstrate the effectiveness of our DHOT-GM method, we verify it on the attribute graph matching task compared with baselines. We select 7 unsupervised graph matching methods. Among these methods, UniAlign [17] is QAP-based, REGAL [12], WAlign [9], and GAlign [34] are node embedding-based, and GWL [42], FGW [36], SLOtAlign [33] are OT-based. To demonstrate the advantages of DHOT-GM as an unsupervised method, we also select 4 semi-supervised graph matching baselines for comparison, i.e., IsoRank [29], FINAL [50], DeepLink [54] and CENALP [7].

Table 1: Description of the datasets.

Dataset	#Nodes	#Edges	Dim. of Attr.
Douban Online-Offline	3,906	16,328	538
	1,128	3,022	538
ACM-DBLP	9,872	39,561	17
	9,916	44,808	17
PPI	1,767	17,042	50
Cora	2,708	5,278	1,433

Table 2: Comparison for the read-world graph matching on the node correctness (%) and runtime (second). For each dataset, we bold the best result in each methodological category and highlight the global optimal performance in red.

Type		semi-supervised				unsupervised							
Method		IsoRank	FINAL	DeepLink	CENALP	UniAlign	REGAL	GAlign	WAlign	GWL	FGW	SLOTAlign	DHOT-GM
ACM-DBLP	NC@1	17.09	30.25	12.19	<b>34.81</b>	0.08	3.49	58.43	63.91	4.02	49.11	65.52	<b>68.11</b>
	NC@5	35.42	<b>55.32</b>	32.98	51.86	0.41	9.74	78.78	83.86	5.96	52.06	84.05	<b>85.75</b>
	NC@10	47.11	<b>67.95</b>	44.58	62.23	0.91	13.61	84.46	89.12	7.34	52.09	87.76	<b>90.25</b>
	Time(s)	208.5	472.4	2369.3	20296.3	19.8	540.3	213.4	672.6	828.7	106.8	539.4	1435.7
Douban Online-Offline	NC@1	30.86	<b>52.24</b>	8.86	23.70	0.63	1.97	44.10	39.53	0.27	<b>58.86</b>	49.91	54.03
	NC@5	50.09	<b>89.80</b>	22.36	38.10	3.49	6.44	67.98	61.63	0.72	63.23	<b>74.69</b>	74.06
	NC@10	61.27	<b>95.97</b>	30.95	43.56	8.23	10.11	77.73	71.02	1.07	63.69	79.43	<b>80.59</b>
	Time(s)	5.4	134.9	286.1	1023.8	1.5	69.5	45.5	43.9	25.1	83.3	13.5	41.2
PPI	NC@1	17.71	<b>38.09</b>	10.36	28.35	0.68	6.68	67.18	64.63	11.38	83.32	76.63	<b>86.98</b>
	NC@5	28.64	<b>52.91</b>	14.94	41.43	2.77	18.11	78.49	73.23	13.30	83.32	82.06	<b>91.06</b>
	NC@10	34.75	<b>55.35</b>	18.05	47.82	4.92	25.69	82.57	76.91	16.07	83.32	83.76	<b>92.19</b>
	Time(s)	6.1	3.6	624.9	1546.7	1.9	28.8	18.3	45.8	14.9	5.3	8.1	31.3
Cora	NC@1	16.88	67.25	10.86	<b>76.55</b>	0.41	5.50	98.38	93.72	0.03	99.19	98.86	<b>99.45</b>
	NC@5	34.12	81.35	27.81	<b>86.85</b>	1.85	11.11	99.85	96.01	0.11	99.19	99.89	<b>100.00</b>
	NC@10	42.95	85.52	36.34	<b>88.81</b>	3.91	14.73	99.96	96.38	0.37	99.19	99.89	<b>100.00</b>
	Time(s)	43.9	353.8	1449.1	3128.2	1.9	50.3	30.8	109.9	27.7	4.7	22.5	78.7

Note that these baselines require a prior matching matrix or matching node pairs as training labels. We use 10% of the ground-truth when implementing the semi-supervised methods. All the experiments are implemented in PyTorch and conducted on NVIDIA GeForce RTX 3090.

#### 4.1.2 Datasets

We evaluate baselines and our DHOT-GM on two datasets and each dataset contains one or two real-world graphs with their topology and attribute information. Table 1 shows the statistics of the datasets. Details for datasets are described below.

- ACM-DBLP [50] is a two co-authorship networks dataset for publication information. The ACM network includes 9,916 authors and 44,808 co-authorships, while the DBLP network includes 9,872 authors and 39,561 co-authorships. Node attributes are composed of the number of papers published by the author in 17 locations. The 6,325 co-authors in the two networks constitute the ground-truth matching node pairs.
- Douban Online-Offline [51] includes an online graph with 16,328 interactions among 3,906 users and an offline graph with 3,022 interactions among 1,118 users. The user’s location represents node attributes. The ground-truth matching is the 1,118 users appearing in both graphs.
- Cora [45] is a citation network where nodes mean publications and edges mean citation relationships. It includes 2,708 nodes and 5,278 edges and each node has 1,433 attributes.
- PPI [55] is a protein-protein interaction network dataset containing 24 graphs. We select the first graph which contains 1,767 nodes with 50 attributes and 17,042 edges for our task.

Since Cora and PPI only contain one graph, we generate the other graph by cutting  $E\%$  edges in the original graph randomly and adding  $E\%$  random edges accordingly. Here,  $E \in \{10, 20, \dots, 60\}$ , indicating different noise levels.

### 4.1.3 Metrics

We evaluate the performance of different methods by the commonly used top-K node correctness NC@K in the literature. Given a node of the graph  $\mathcal{G}_s$ , NC@K takes the most similar K nodes from all possible matching in the graph  $\mathcal{G}_t$  as a Top-K list, and finally calculates the percentage of ground-truth matching in the list.

## 4.2 Numerical Comparisons

### 4.2.1 Node Correctness and Runtime

We first show the matching performance of DHOT-GM on the real-world graph matching task. In Table 2, it can be observed that DHOT-GM achieves the best results on ACM-DBLP, PPI, and Cora. For Douban Online-Offline, although DHOT-GM is slightly lower than FGW on NC@1, it outperforms all the unsupervised methods on NC@10. We believe that this phenomenon is due to the large disparity in the number of nodes in Douban Online-Offline, and the information imbalance between modalities is more serious, which makes it difficult to achieve exact matching without prior knowledge. However, even in this case, DHOT-GM still outperforms FINAL which is the best in semi-supervised methods on NC@1. This shows that DHOT-GM remains competitive with the semi-supervised methods in an imbalanced situation of nodes. In addition, we note that the performance of some unsupervised baselines like UniAlign, REGAL, and GWL is poor on all datasets, which is because all these methods consider mainly the graph topology for matching, and lack effective utilization of node attributes. We also compare the runtime of DHOT-GM and baselines and DHOT-GM is comparable in efficiency to existing unsupervised graph matching methods.

### 4.2.2 Robustness to Noise

Furthermore, we also investigate the impact of noise on DHOT-GM. Taking the PPI dataset as an example, we continuously increase the ratio of randomly reconnected edges to generate the graph. In Figure 3, we observe that DHOT-GM still shows significant performance even after 60% of edges are affected by noise, while other unsupervised methods that perform well at low noise levels cannot guarantee this. This indicates that DHOT-GM has strong robustness at high noise levels.

## 4.3 Ablation Study

### 4.3.1 The Number of Modalities

We first investigate the matching performance of DHOT-GM with different numbers of graph modalities selected. As shown in Table 3, the performance on ACM-DBLP increases with the number of modalities. This shows that DHOT-GM is able to fully utilize the matching results between multiple modalities of two graphs on this dataset. On Douban Online-Offline, we observe that the highest performance is achieved when the number of modalities is equal to 3. Continuing to increase the number of modalities leads to a decrease in performance instead. We believe that the number of nodes between the two graphs in Douban Online-Offline is unbalanced, which leads to more significant differences between their modalities and thus makes it more difficult to match.

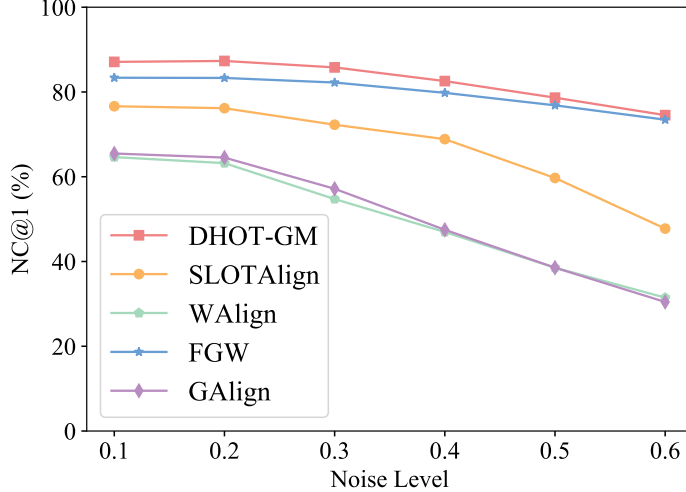


Figure 3: Results under different noise levels on PPI dataset.

Table 3: Effects of the number of modalities.

$K$	ACM-DBLP			Douban Online-Offline		
	NC@1	NC@5	NC@10	NC@1	NC@5	NC@10
2	66.62	85.61	89.96	41.14	57.16	60.29
3	68.11	85.75	90.25	<b>54.03</b>	<b>74.06</b>	<b>80.59</b>
4	<b>68.95</b>	<b>86.53</b>	<b>90.28</b>	47.32	72.81	76.92

#### 4.3.2 The Contribution of Different Modalities

To further explore which modality can most affect the performance of graph matching, we also conduct experiments for DHOT-GM through pairwise combinations of 3 modalities. Results in Table 4 show that on the ACM-DBLP dataset, the node attributes are necessary for the matching performance, but on Douban Online-Offline, the graph topology is essential. This indicates that for the attribute graph matching task, the matching performance is controlled by different modalities in different dataset scenarios.

#### 4.3.3 The Learning Rate of Marginal Update

We also explore the impact of the learning rate of the marginal update. We take the value of the learning rate  $\gamma$  from  $\{0, 0.01, 0.05, 0.1, 0.5, 1\}$ . It is observed that DHOT-GM has a tendency to improve the performance on both datasets as the learning rate gradually increases in Table 5. This phenomenon is consistent with our initial assumption that the matching result between different modalities has different significance. Learnable weights for different modalities can achieve better matching performance than assigning the same uniform distribution to each modality.

#### 4.3.4 The Rationality of Using Cross-modal Matching

We visualize the learned OT matrices by DHOT-GM for different datasets. In Figure 4, we discover that the weight for graph topology matching is dominant on the ACM-DBLP and Douban Online-Offline datasets, while on the PPI and Cora datasets, the OT matrices for modalities are more balanced. We believe this is because on the ACM-DBLP and Douban Online-Offline datasets, the differences between the two graphs are greater in the node attributes and subgraph structures,

Table 4: Ablation study on using different modalities.

Used Modalities	ACM-DBLP			Douban Online-Offline		
	NC@1	NC@5	NC@10	NC@1	NC@5	NC@10
Topology + Attribute	66.97	85.34	89.36	41.14	57.16	60.29
Topology + Subgraph	0.46	1.42	2.48	34.53	58.14	63.69
Attribute + Subgraph	33.33	54.50	63.76	5.01	11.54	18.07
All	<b>68.11</b>	<b>85.75</b>	<b>90.25</b>	<b>54.03</b>	<b>74.06</b>	<b>80.59</b>

Table 5: Effects of updating marginals.

$\gamma$	ACM-DBLP			Douban Online-Offline		
	NC@1	NC@5	NC@10	NC@1	NC@5	NC@10
0	61.34	84.41	89.22	24.96	56.62	66.46
0.01	64.79	84.60	89.30	24.87	56.71	66.01
0.05	65.52	84.77	89.28	26.12	56.62	65.74
0.1	56.4	84.52	89.12	28.71	59.12	67.62
0.5	67.73	85.63	89.74	38.28	68.96	75.04
1.0	<b>68.11</b>	<b>85.75</b>	<b>90.25</b>	<b>54.03</b>	<b>74.06</b>	<b>80.59</b>

whereas the graph topology is based only on the adjacency matrix so it provides the main performance in graph matching. However, on the PPI and Cora datasets, we generate a noisy version of the original graph, so the relational matrices of the two are closer for each modality, and effective matching results can be provided between different modalities. We further visualize the results of some cross-modal relational matrices matching in Figure 5 on PPI and Cora, and observe that they exhibit a similar diagonal structure to the ground-truth. This phenomenon indicates that DHOT-GM can effectively utilize the potential of cross-modal matching.

#### 4.3.5 The Rationality of Only Using Low-pass Relational Matrices

As aforementioned in Section 3.2, the relational matrices corresponding to the subgraph structures, i.e.,  $\{\mathbf{D}^k\}_{k=3}^K$ , are achieved by passing the node attributes through low-pass graph filters iteratively and computing their inner products. Then, a question arises — can we derive the relational matrices by high-pass graph filtering (e.g., constructing  $\mathbf{D}_H = \hat{\mathbf{L}}\mathbf{X}(\hat{\mathbf{L}}\mathbf{X})^\top$ , where  $\hat{\mathbf{L}}$  is the normalized graph Laplacian matrix)? In our opinion, applying such high-pass relational matrices to graph matching tasks may be inappropriate. In particular, graph matching is naturally sensitive to the topological noise (e.g., the random connections and disconnections of edges) in graphs [34, 33], while the high-pass graph filtering encodes the discrepancy of node attributes along graph edges, whose output is largely influenced by the noise of the edges. As a result, the high-pass relational matrix  $\mathbf{D}_H$  amplifies the topological noise of the graph, and matching graphs based on their  $\mathbf{D}_H$ ’s often leads to undesired results.

To verify the above claim, we explore the impact of the high-pass relational matrices on the performance of DHOT-GM, constructing a new multi-modal relational matrix set  $\mathcal{D}_{new} = \mathcal{D} \cup \{\mathbf{D}_H\}$  and implementing our DHOT-GM method accordingly. The results in Table 6 show that applying  $\mathbf{D}_H$  results in the performance degradation. Additionally, because of the noise within it, DHOT-GM encounters numerical issues under the original parameter settings — the proximal gradient algorithm suffers from the numerical instability when computing the GW distance relevant to  $\mathbf{D}_H$ .

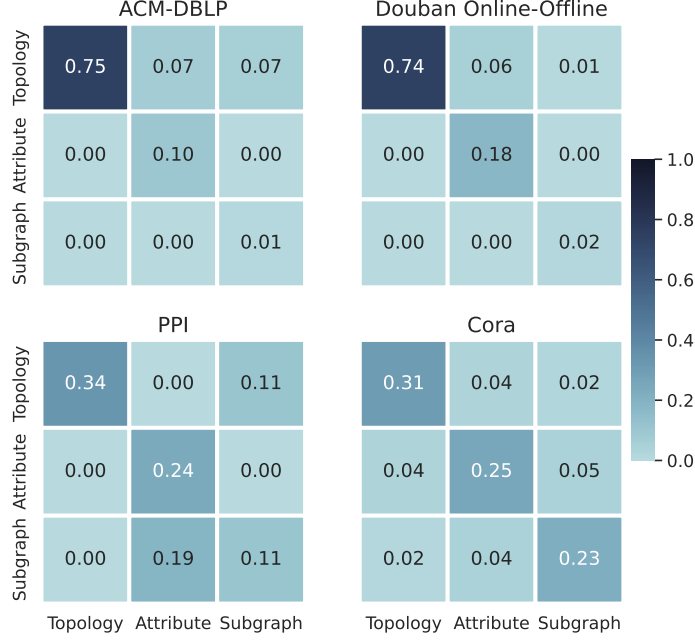


Figure 4: The upper-level OT matrices (i.e.,  $\Theta$ 's) learned for different datasets.

Table 6: Ablation study on adding high-pass mechanism.

Relational matrix set	Original #Epochs			Reduced #Epochs		
	NC@1	NC@5	NC@10	NC@1	NC@5	NC@10
Original $\mathcal{D}$	54.03	74.06	80.59	35.42	59.75	64.58
$\mathcal{D} \cup \{\mathcal{D}_H\}$	NaN	NaN	NaN	32.02	57.96	62.79

## 5 Conclusion

In this work, we propose a novel DHOT framework for graph matching using multi-modal information from graphs. Given the multi-modal relational matrices of graphs, the proposed framework makes attempts to leverage the cross-modal matching results and demonstrate their usefulness. The experimental results show that our method can achieve encouraging performance in unsupervised attribute graph matching.

In the future, we plan to explore the impact of modal imbalance on graph matching performance, making the framework more robust and scalable when dealing with different source and target graph structures. At the same time, we also hope to reduce duplicate calculations of unimportant modal information, thereby improving the efficiency of the algorithm.

## References

- [1] D. Alvarez-Melis, T. Jaakkola, and S. Jegelka. Structured optimal transport. In *International conference on artificial intelligence and statistics*, pages 1771–1780. PMLR, 2018.
- [2] T. S. Caetano, J. J. McAuley, L. Cheng, Q. V. Le, and A. J. Smola. Learning graph matching. *IEEE transactions on pattern analysis and machine intelligence*, 31(6):1048–1058, 2009.



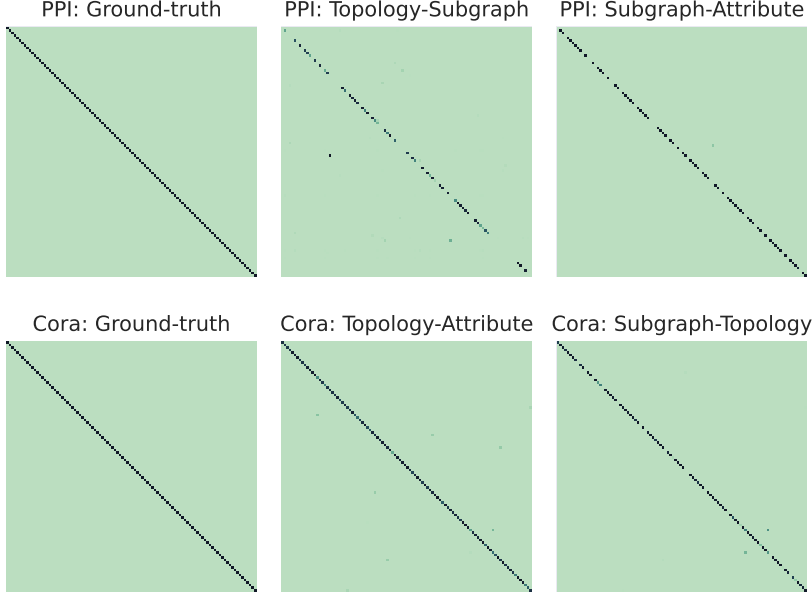


Figure 5: The lower-level OT matrices (i.e.,  $T^{(p,q)}$ 's) for nodes across different modalities. For the convenience of visualization, we take the first 100 nodes for all datasets. The darker the color, the higher the value.

- [3] L. Chen, Z. Gan, Y. Cheng, L. Li, L. Carin, and J. Liu. Graph optimal transport for cross-domain alignment. In *International Conference on Machine Learning*, pages 1542–1553. PMLR, 2020.
- [4] Y. Chen, T. T. Georgiou, and A. Tannenbaum. Optimal transport for gaussian mixture models. *IEEE Access*, 7:6269–6278, 2018.
- [5] M. Cuturi. Sinkhorn distances: Lightspeed computation of optimal transport. In C. J. C. Burges, L. Bottou, Z. Ghahramani, and K. Q. Weinberger, editors, *Advances in Neural Information Processing Systems 26: 27th Annual Conference on Neural Information Processing Systems 2013. Proceedings of a meeting held December 5-8, 2013, Lake Tahoe, Nevada, United States*, pages 2292–2300, 2013.
- [6] M. Defferrard, X. Bresson, and P. Vandergheynst. Convolutional neural networks on graphs with fast localized spectral filtering. *Advances in neural information processing systems*, 29, 2016.
- [7] X. Du, J. Yan, and H. Zha. Joint link prediction and network alignment via cross-graph embedding. In S. Kraus, editor, *Proceedings of the Twenty-Eighth International Joint Conference on Artificial Intelligence, IJCAI 2019, Macao, China, August 10-16, 2019*, pages 2251–2257. ijcai.org, 2019.
- [8] M. Fey, J. E. Lenssen, C. Morris, J. Masci, and N. M. Kriege. Deep graph matching consensus. In *8th International Conference on Learning Representations, ICLR 2020, Addis Ababa, Ethiopia, April 26-30, 2020*. OpenReview.net, 2020.
- [9] J. Gao, X. Huang, and J. Li. Unsupervised graph alignment with wasserstein distance discriminator. In *Proceedings of the 27th ACM SIGKDD Conference on Knowledge Discovery & Data Mining*, pages 426–435, 2021.

- [10] A. Genevay, G. Peyré, and M. Cuturi. Learning generative models with sinkhorn divergences. In *International Conference on Artificial Intelligence and Statistics*, pages 1608–1617. PMLR, 2018.
- [11] S. Hashemifar, Q. Huang, and J. Xu. Joint alignment of multiple protein–protein interaction networks via convex optimization. *Journal of Computational Biology*, 23(11):903–911, 2016.
- [12] M. Heimann, H. Shen, T. Safavi, and D. Koutra. REGAL: representation learning-based graph alignment. In A. Cuzzocrea, J. Allan, N. W. Paton, D. Srivastava, R. Agrawal, A. Z. Broder, M. J. Zaki, K. S. Candan, A. Labrinidis, A. Schuster, and H. Wang, editors, *Proceedings of the 27th ACM International Conference on Information and Knowledge Management, CIKM 2018, Torino, Italy, October 22-26, 2018*, pages 117–126. ACM, 2018.
- [13] B. Hooi, K. Shin, H. A. Song, A. Beutel, N. Shah, and C. Faloutsos. Graph-based fraud detection in the face of camouflage. *ACM Transactions on Knowledge Discovery from Data (TKDD)*, 11(4):1–26, 2017.
- [14] M. Huang, Y. Liu, X. Ao, K. Li, J. Chi, J. Feng, H. Yang, and Q. He. Auc-oriented graph neural network for fraud detection. In *Proceedings of the ACM Web Conference 2022*, pages 1311–1321, 2022.
- [15] L. V. Kantorovich. On the translocation of masses. In *Dokl. Akad. Nauk. USSR (NS)*, volume 37, pages 199–201, 1942.
- [16] T. N. Kipf and M. Welling. Semi-supervised classification with graph convolutional networks. In *5th International Conference on Learning Representations, ICLR 2017, Toulon, France, April 24-26, 2017, Conference Track Proceedings*. OpenReview.net, 2017.
- [17] D. Koutra, H. Tong, and D. Lubensky. Big-align: Fast bipartite graph alignment. In *2013 IEEE 13th international conference on data mining*, pages 389–398. IEEE, 2013.
- [18] J. Lee, M. Dabagia, E. Dyer, and C. Rozell. Hierarchical optimal transport for multimodal distribution alignment. *Advances in neural information processing systems*, 32, 2019.
- [19] C. Li, S. Wang, H. Wang, Y. Liang, P. S. Yu, Z. Li, and W. Wang. Partially shared adversarial learning for semi-supervised multi-platform user identity linkage. In W. Zhu, D. Tao, X. Cheng, P. Cui, E. A. Rundensteiner, D. Carmel, Q. He, and J. X. Yu, editors, *Proceedings of the 28th ACM International Conference on Information and Knowledge Management, CIKM 2019, Beijing, China, November 3-7, 2019*, pages 249–258. ACM, 2019.
- [20] C. Li, S. Wang, P. S. Yu, L. Zheng, X. Zhang, Z. Li, and Y. Liang. Distribution distance minimization for unsupervised user identity linkage. In A. Cuzzocrea, J. Allan, N. W. Paton, D. Srivastava, R. Agrawal, A. Z. Broder, M. J. Zaki, K. S. Candan, A. Labrinidis, A. Schuster, and H. Wang, editors, *Proceedings of the 27th ACM International Conference on Information and Knowledge Management, CIKM 2018, Torino, Italy, October 22-26, 2018*, pages 447–456. ACM, 2018.
- [21] X. Liu, H. Hong, X. Wang, Z. Chen, E. Kharlamov, Y. Dong, and J. Tang. Selfkg: self-supervised entity alignment in knowledge graphs. In *Proceedings of the ACM Web Conference 2022*, pages 860–870, 2022.
- [22] Y. Liu, H. Ding, D. Chen, and J. Xu. Novel geometric approach for global alignment of PPI networks. In S. P. Singh and S. Markovitch, editors, *Proceedings of the Thirty-First AAAI Conference on Artificial Intelligence, February 4-9, 2017, San Francisco, California, USA*, pages 31–37. AAAI Press, 2017.

- [23] E. M. Loiola, N. M. M. De Abreu, P. O. Boaventura-Netto, P. Hahn, and T. Querido. A survey for the quadratic assignment problem. *European journal of operational research*, 176(2):657–690, 2007.
- [24] D. Luo, H. Xu, and L. Carin. Differentiable hierarchical optimal transport for robust multi-view learning. *IEEE Transactions on Pattern Analysis and Machine Intelligence*, 2022.
- [25] F. Mémoli. Gromov–wasserstein distances and the metric approach to object matching. *Foundations of computational mathematics*, 11:417–487, 2011.
- [26] G. Peyré, M. Cuturi, and J. Solomon. Gromov-wasserstein averaging of kernel and distance matrices. In M. Balcan and K. Q. Weinberger, editors, *Proceedings of the 33rd International Conference on Machine Learning, ICML 2016, New York City, NY, USA, June 19-24, 2016*, volume 48 of *JMLR Workshop and Conference Proceedings*, pages 2664–2672. JMLR.org, 2016.
- [27] M. Scetbon, G. Peyré, and M. Cuturi. Linear-time gromov wasserstein distances using low rank couplings and costs. In *International Conference on Machine Learning*, pages 19347–19365. PMLR, 2022.
- [28] B. Schmitzer and C. Schnörr. A hierarchical approach to optimal transport. In *International conference on scale space and variational methods in computer vision*, pages 452–464. Springer, 2013.
- [29] R. Singh, J. Xu, and B. Berger. Global alignment of multiple protein interaction networks with application to functional orthology detection. *Proceedings of the National Academy of Sciences*, 105(35):12763–12768, 2008.
- [30] J. Solomon, G. Peyré, V. G. Kim, and S. Sra. Entropic metric alignment for correspondence problems. *ACM Transactions on Graphics (ToG)*, 35(4):1–13, 2016.
- [31] B. Su and G. Hua. Order-preserving wasserstein distance for sequence matching. In *Proceedings of the IEEE conference on computer vision and pattern recognition*, pages 1049–1057, 2017.
- [32] Z. Sun, Q. Zhang, W. Hu, C. Wang, M. Chen, F. Akrami, and C. Li. A benchmarking study of embedding-based entity alignment for knowledge graphs. *ArXiv preprint*, abs/2003.07743, 2020.
- [33] J. Tang, W. Zhang, J. Li, K. Zhao, F. Tsung, and J. Li. Robust attributed graph alignment via joint structure learning and optimal transport. *ArXiv preprint*, abs/2301.12721, 2023.
- [34] H. T. Trung, T. Van Vinh, N. T. Tam, H. Yin, M. Weidlich, and N. Q. V. Hung. Adaptive network alignment with unsupervised and multi-order convolutional networks. In *2020 IEEE 36th International Conference on Data Engineering (ICDE)*, pages 85–96. IEEE, 2020.
- [35] S. Umeyama. An eigendecomposition approach to weighted graph matching problems. *IEEE transactions on pattern analysis and machine intelligence*, 10(5):695–703, 1988.
- [36] T. Vayer, N. Courty, R. Tavenard, L. Chapel, and R. Flamary. Optimal transport for structured data with application on graphs. In K. Chaudhuri and R. Salakhutdinov, editors, *Proceedings of the 36th International Conference on Machine Learning, ICML 2019, 9-15 June 2019, Long Beach, California, USA*, volume 97 of *Proceedings of Machine Learning Research*, pages 6275–6284. PMLR, 2019.
- [37] M. Vento and P. Foggia. Graph matching techniques for computer vision. In *Image Processing: Concepts, Methodologies, Tools, and Applications*, pages 381–421. IGI Global, 2013.
- [38] C. Vincent-Cuaz, T. Vayer, R. Flamary, M. Corneli, and N. Courty. Online graph dictionary learning. In M. Meila and T. Zhang, editors, *Proceedings of the 38th International Conference on Machine Learning, ICML 2021, 18-24 July 2021, Virtual Event*, volume 139 of *Proceedings of Machine Learning Research*, pages 10564–10574. PMLR, 2021.

- [39] Y. Xie, Y. Mao, S. Zuo, H. Xu, X. Ye, T. Zhao, and H. Zha. A hypergradient approach to robust regression without correspondence. In *International Conference on Learning Representations*, 2020.
- [40] H. Xu. Gromov-wasserstein factorization models for graph clustering. In *The Thirty-Fourth AAAI Conference on Artificial Intelligence, AAAI 2020, The Thirty-Second Innovative Applications of Artificial Intelligence Conference, IAAI 2020, The Tenth AAAI Symposium on Educational Advances in Artificial Intelligence, EAAI 2020, New York, NY, USA, February 7-12, 2020*, pages 6478–6485. AAAI Press, 2020.
- [41] H. Xu, D. Luo, and L. Carin. Scalable gromov-wasserstein learning for graph partitioning and matching. In H. M. Wallach, H. Larochelle, A. Beygelzimer, F. d’Alché-Buc, E. B. Fox, and R. Garnett, editors, *Advances in Neural Information Processing Systems 32: Annual Conference on Neural Information Processing Systems 2019, NeurIPS 2019, December 8-14, 2019, Vancouver, BC, Canada*, pages 3046–3056, 2019.
- [42] H. Xu, D. Luo, H. Zha, and L. Carin. Gromov-wasserstein learning for graph matching and node embedding. In K. Chaudhuri and R. Salakhutdinov, editors, *Proceedings of the 36th International Conference on Machine Learning, ICML 2019, 9-15 June 2019, Long Beach, California, USA*, volume 97 of *Proceedings of Machine Learning Research*, pages 6932–6941. PMLR, 2019.
- [43] Y. Yan, S. Zhang, and H. Tong. Bright: A bridging algorithm for network alignment. In *Proceedings of the Web Conference 2021*, pages 3907–3917, 2021.
- [44] J. Yang, Y. Liu, and H. Xu. Hotnas: Hierarchical optimal transport for neural architecture search. In *Proceedings of the IEEE/CVF Conference on Computer Vision and Pattern Recognition*, pages 11990–12000, 2023.
- [45] Z. Yang, W. W. Cohen, and R. Salakhutdinov. Revisiting semi-supervised learning with graph embeddings. In M. Balcan and K. Q. Weinberger, editors, *Proceedings of the 33rd International Conference on Machine Learning, ICML 2016, New York City, NY, USA, June 19-24, 2016*, volume 48 of *JMLR Workshop and Conference Proceedings*, pages 40–48. JMLR.org, 2016.
- [46] M. Yurochkin, S. Clatici, E. Chien, F. Mirzazadeh, and J. M. Solomon. Hierarchical optimal transport for document representation. *Advances in neural information processing systems*, 32, 2019.
- [47] A. Zanfir and C. Sminchisescu. Deep learning of graph matching. In *Proceedings of the IEEE conference on computer vision and pattern recognition*, pages 2684–2693, 2018.
- [48] M. Zaslavskiy, F. Bach, and J.-P. Vert. A path following algorithm for the graph matching problem. *IEEE Transactions on Pattern Analysis and Machine Intelligence*, 31(12):2227–2242, 2008.
- [49] Z. Zeng, S. Zhang, Y. Xia, and H. Tong. Parrot: Position-aware regularized optimal transport for network alignment. In *Proceedings of the ACM Web Conference 2023*, pages 372–382, 2023.
- [50] S. Zhang and H. Tong. FINAL: fast attributed network alignment. In B. Krishnapuram, M. Shah, A. J. Smola, C. C. Aggarwal, D. Shen, and R. Rastogi, editors, *Proceedings of the 22nd ACM SIGKDD International Conference on Knowledge Discovery and Data Mining, San Francisco, CA, USA, August 13-17, 2016*, pages 1345–1354. ACM, 2016.
- [51] S. Zhang and H. Tong. Attributed network alignment: Problem definitions and fast solutions. *IEEE Transactions on Knowledge and Data Engineering*, 31(9):1680–1692, 2018.

- [52] S. Zhang, H. Tong, L. Jin, Y. Xia, and Y. Guo. Balancing consistency and disparity in network alignment. In *Proceedings of the 27th ACM SIGKDD conference on knowledge discovery & data mining*, pages 2212–2222, 2021.
- [53] F. Zhou and F. D. la Torre. Factorized graph matching. In *2012 IEEE Conference on Computer Vision and Pattern Recognition, Providence, RI, USA, June 16-21, 2012*, pages 127–134. IEEE Computer Society, 2012.
- [54] F. Zhou, L. Liu, K. Zhang, G. Trajcevski, J. Wu, and T. Zhong. Deeplink: A deep learning approach for user identity linkage. In *IEEE INFOCOM 2018-IEEE conference on computer communications*, pages 1313–1321. IEEE, 2018.
- [55] M. Zitnik and J. Leskovec. Predicting multicellular function through multi-layer tissue networks. *Bioinformatics*, 33(14):i190–i198, 2017.